Automation in Construction 82 (2017) 166–178

Contents lists available at ScienceDirect

Automation in Construction

journal homepage: www.elsevier.com/locate/autcon

Collective sensing of workers' gait patterns to identify fall hazards in construction

Kanghyeok Yang[a], Changbum R. Ahn[c,*], Mehmet C. Vuran[b], Hyunsoo Kim[a]

[a] Charles Durham School of Architectural Engineering and Construction, University of Nebraska–Lincoln, W113 Nebraska Hall, Lincoln, NE 68588, United States
[b] Department of Computer Science and Engineering, University of Nebraska–Lincoln, 214 Schorr Center, Lincoln, NE 68588, United States
[c] Department of Construction Science, Texas A & M University, 330B Francis Hall, 3137 TAMU, College Station, TX 77843-3137, United States

ARTICLE INFO

Keywords:
Construction safety
Hazard identification
Slips, trips, and falls
Gait analysis
Wearable inertial measurement units

ABSTRACT

Current hazard-identification efforts in construction mostly rely on human judgment, a reality that leaves a significant number of hazards unidentified or not well-assessed. This situation highlights a need for enhancing hazard-identification capabilities in dynamic and unpredictable construction environments. Given the fact that hazards cause disruptions in workers' behaviors and responses, capturing such disruptions offers opportunities for identifying hazards. This study proposes a collective sensing approach that senses and assesses workers' gait abnormalities in order to identify physical fall hazards in a construction jobsite. Laboratory experiments simulating an ironworkers' working environment were designed and conducted to examine the feasibility of the proposed approach. A wearable inertial measurement unit (WIMU) attached to a subject's ankle collected kinematic gait data. The results indicated that the aggregated gait abnormality score from multiple subjects have a strong correlation with the existence of installed fall hazards such as obstacles and slippery surfaces. This outcome highlights the opportunity for future devices to use workers' abnormal gait responses to reveal safety hazards in construction environments.

1. Introduction

The development of wearable sensing technology enables the collection and analysis of individual worker's bodily and physiological responses to work on a job site, an opportunity that was previously unattainable [1–3]. Collecting and analyzing worker's data is especially valuable in the pursuit of increasing safety on a construction site since identifying at-risk workers and safety hazards represents the first step towards mitigating risks. The hazard identification in a construction environment is still a challenging issue due to the lack of resources [4] and the dynamic work environments involved [5]. Construction takes place both indoor and outdoor—often at the same time—and tasks often generate unpredictable work environments such as surface contamination by dust and mud [5]. Different also tasks take place in the same space [5], which yields frequent overlaps in the construction work environment and site changes due to the interaction between various activities. With such dynamic environments, construction sites contain a significant quantity of unidentified or not well-assessed hazards that expose construction workers to additional safety risks during required operations [6,7].

The standard approach to identifying a hazard in construction mainly functions on the basis of the judgment of safety managers or individual workers [6]. However, these approaches still encounter three main challenges in a construction environment: 1) Safety managers must assess multiple areas, a fact that decreases their effectiveness in addressing new safety risks as hazards arise; 2) individuals have different levels of knowledge and experience in identifying hazards; 3) dynamic work environments add complexities that decrease individuals' ability to recognize hazards on the jobsite. Therefore, innovative approaches to identifying hazards would help address such limitations and enhance hazard-identification capabilities to prevent accidents in a construction site.

Among the various types of accidents, slips, trips and falls (STFs) are the primary sources of injuries among construction workers [8,9], and these events result in enormous economic and human losses [10]. With such high risk of STFs, many previous studies have sought to automatically detect STFs through wearable sensing technology [11–15]. In clinical spheres, Bourke and his colleagues developed a threshold-based fall-detection algorithm that uses an accelerometer [11] or gyroscope [12]; their research showed a feasibility of automated detection of fall of patients with wearable sensor. Lai et al. [13] proposed a method for detecting patients' injuries using multiple accelerometers; their

* Corresponding author.
E-mail addresses: kyang12@huskers.unl.edu (K. Yang), cahn2@unl.edu, ryanahn@tamu.edu (C.R. Ahn), mcvuran@cse.unl.edu (M.C. Vuran), hkim13@unl.edu (H. Kim).

http://dx.doi.org/10.1016/j.autcon.2017.04.010
Received 1 August 2016; Received in revised form 6 April 2017; Accepted 7 April 2017
Available online 29 April 2017

outcomes revealed an opportunity of identifying injured body area and estimating severity through data from accelerometers. In the construction-safety realm, Lim et al. [14] implemented an artificial neural network model to detect slip and trip events using acceleration data recovered from a smartphone. Dzeng et al. [15] investigated whether it was possible to detect fall portents—*i.e.*, near-miss falls—using embedded IMU sensors in a smartphone. Combined, these studies reveal the feasibility of using wearable sensors to detect occurred STFs in both daily-living or working environments. However, considering the fact that not all fall hazards will result in STFs, current approaches based on retrospectives have limited performance for robust identification of current hazards or future risks. Thereby, different approach that can identify a possible source of STFs (*i.e.*, fall hazards) without experiencing STFs would be necessary to increase the hazard identification performance in construction.

Previous studies revealed that the human body responds to physical environmental changes [16,17]. Accordingly, considering the fact that STFs often begin with bad interactions between a foot and floor-surface conditions, potential sources of STFs could foreseeably be identified by studying changes in a worker's gait pattern (*i.e.*, foot movement patterns) alongside the changes' spatial locations. In this context, this study investigates whether and how measuring workers' gait patterns can help locate fall hazards in a construction jobsite. Specifically, this study used wearable inertial measurement units (WIMU) to collect workers' gait patterns as the subjects responded to fall hazards in a laboratory settings and then computed spatiotemporal gait features to quantify the workers' gait-pattern changes. In order to effectively translate the degree of gait disruption from multiple gait features into a single value, this study defined an IMU-based Gait Abnormality Score (I-GAS); this score first uses the Mahalanobis distance [18] to measure the magnitude of gait disruption generated from fall hazards and then compares the outcome to reference gait data from non-hazardous locations/laboratory setups. Using the different laboratory experimental setups—-which simulated ironwork environments—this study verified the existence of gait disruptions at hazard location and showed the feasibility of identifying fall hazards using the proposed I-GAS. Consequently, the results of this study contribute to identifying fall hazards in a proactive manner. The developed technique can thereby help construction managers eliminate the risk of hazards without depending exclusively upon observations or hazard reporting from a construction worker.

2. Research background

Fall accidents are the leading cause of fatalities and account for approximately 30% of all fatalities in construction [19]. Also, falls are one of the major causes of minor injuries in construction, and many workers have suffered a significant number of work disabilities (*e.g.*, contusions and fractures) from fall accidents [20]. Due to the high risks and related costs associated with fall accidents, many studies have sought to reveal and prevent the causes of falls in construction [20–23]. Courtney et al. [20] investigated disabling injuries in construction and identified the sources and types of worker injuries from falls. Cattledge et al. [21] analyzed nonfatal injuries from falls in construction and revealed that ladder and scaffold tasks are major sources of such injuries—these activities account for 50% of all nonfatal fall injuries in construction. Huang et al. [22] analyzed fall-accident records and identified high-risk trades, causes of accidents and other related information (*e.g.*, types of construction projects, fall height, worker's age, height of fall) in construction. Chi et al. [23] identified contributing factors of fatal fall accidents in construction and suggested prevention measures for fall accidents. These studies provide valuable insights about fall-causing environments and situations in construction.

However, hazard identification still relies on individuals' hazard-recognition abilities, which may vary according to experience and knowledge of hazards. In response, previous studies into hazard identification worked to increase individuals' recognition abilities through training programs or training in virtual environments [24–26]. Albert et al. [24] developed a maturity model for enhancing the hazard-recognition capabilities of construction workers and demonstrated the usefulness of the model by observing increases in hazard-recognition levels during construction. Bahn [25] studied the hazard-identification levels of construction workers and showed that length of work experience did not predetermine the hazard-identification performance of an individual. Sacks et al. [26] tested safety training in a virtual construction site and showed the effectiveness of using a virtual reality environment for worker's safety training. Each of these studies helped reveal the significance of worker training and preparation in construction safety.

While training is an effective way to enhance workers' hazard-identification performance, humans' recognition abilities are still subject to surrounding environmental factors (*e.g.*, noise and low light), especially in a dynamic environment such as construction. For example, a slippery surface—which is one of the leading causes of slip events—is challenging to detect in low-light conditions. Also, construction workers often must manually handle material (*e.g.*, carry, pull, or push) during tasks, which often interferes with visibility for hazard identification [5]. Thus, environmental factors during construction can easily undermine current hazard-identification performance, and workers are still at risk of injuries due to unidentified hazards.

It is well-known that existing hazards can cause a certain amount of disruptions in workers' behaviors, and these disruptions can evolve into accidents [27]. Also, falls often begin as a result of unexpected changes between a foot surface and the surface under the foot [28,29]. Thus, fall hazards cause disruptions to workers' gait movements, and these gait-pattern changes can foreseeably provide an insight into the existence of fall hazards. In such circumstances, gait analysis is widely studied to prevent fall accidents or to identify a potential faller in clinical applications [30–34]. In the past, such gait analyses were only available in the laboratory setting using a marker-based motion-tracking system [31,32] or a floor-pressure sensor system [33,34]; however, with the recent developments in wearable sensing technology and analysis techniques, ambulatory gait analysis has become available to outdoor environments through the use of wearable sensor systems. Accordingly, clinical researchers have begun to implement wearable sensor-based gait analysis methodologies to record spatiotemporal gait features (*e.g.*, stride times and stride distances) to then assess the abrupt changes in a patient's gait to measure the risk of falls [35–38]. A single or multiple WIMUs are attached to the subject's lower body parts for ambulatory gait analysis. Then, these sensors record kinematics of leg or foot movements using the accelerometer, gyroscope, and magnetometer imbedded within the WIMU. Previous studies confirmed the accuracy of measuring spatiotemporal gait features using a WIMU and revealed the opportunity for real applications [39–41]. Although these gait analysis techniques have been used to measure the fall risks of patients, no previous studies have used such gait analyses to identify fall hazards in construction environments.

In construction, several studies also used wearable sensing technologies to enhance safety on a construction site while mitigating the difficulties associated with current safety inspections, which depend on human recognition and judgment. Gatti et al. [2] tested a physical monitoring system to measure workers' physiological responses—such as heart rate, breathing rate—for safety monitoring. Cheng et al. [3] proposed the fusion of a location-tracking system and a physiological monitoring system for ergonomic analysis of a construction worker to prevent workers' musculoskeletal or other injuries. Also, different types of sensors, real-time locating systems (RTLS) [42], electromyography (EMG) [43], and electroencephalograms (EEG) [44] were evaluated for identifying hazard proximity and for measuring mental stress and the physical stability of a worker in a construction environment. WIMUs, which include an accelerometer, have been used to monitor a worker's activities and behaviors (*i.e.*, motion tracking) and demonstrated an ability to capture workers' behaviors in construction [45–48]. Joshua

and Varghese [45] proposed an activity-recognizing method that is able to classify construction activities using accelerometer. Jebelli et al. investigated gait stability [46] and posture-stability metrics [47] for measuring the fall risks of construction workers. Valero et al. [48] introduced a system that can detect unsafe postures based on movements of construction worker through WIMU. Combined, these studies demonstrate the applications of this technology to the construction safety realm.

In addition to being inexpensive, small, and durable [47], a WIMU is more robust as compared to vision approaches in challenging conditions such as construction sites [45]. Capitalizing on such advantages in data collection, our previous studies [49–51] detected ironworkers' near-miss falls to identify fall-prone workers and hazardous locations in the ironwork environment. These studies revealed that identified workers' near-miss falls can be used to infer hazardous locations. However, our past studies also identified the challenges in automatically detecting near-misses from sensed data since near-misses are very subjective depending on individual workers. In addition, the low number of near-miss falls that occurred on a jobsite was insufficient to estimate the locations of fall hazards in a quantitative and reliable manner. Our initial study [52] used WIMUs to monitor workers' bodily responses (*e.g.*, body acceleration measured at the waist level) to an environment in order to identify hazards; this preliminary work demonstrated the possibility of using bodily response to identify hazard locations. However, the results of our preliminary work indicated that such an approach required a large amount of sensed data to reliably estimate hazard locations, as bodily responses do not contain direct information about the interaction between a worker's foot and the surface conditions on a jobsite.

In response, this study extends our earlier study [53] and presents gait abnormality–measurement techniques and collective sensing (*i.e.*, data aggregation) techniques for fall-hazard identification. To accomplish this objective, this study measured a breadth of disruptions in a worker's gait due to hazards to identify hazards more efficiently. Due to the fact that fall hazards on a surface directly interact with a worker's foot, this study monitored workers' gait responses by placing WIMUs on subjects' ankles to identify fall hazards concisely. Then, this study comprehensively assessed the deviations among all available gait features to determine instances of gait abnormality. Subsequently, the research team tested the performance of identifying fall hazards by measuring such gait abnormalities. Ultimately, this study validated the proposed approach within a laboratory experiment setting and suggests a potential application of this approach to construction safety management.

3. Methodology

3.1. Data collection during the laboratory experiment

This study conducted a laboratory experiment to collect the disruptions in workers' gaits caused by fall hazards in an ironwork environment, a discipline that records the second highest fatality rates and the highest non-fatal injury rates among construction trades [54]. This study tested two different types of fall hazards (*i.e.*, an obstacle and slippery surface, which are common, observable hazards that can induce slip and trip events). To simulate an ironwork environment, a 24.4 m-long (80 ft-long) steel I-beam structure (see Fig. 1a) was installed 10 cm off the ground. The experiment subjects wore standard safety tools for an ironworker (safety harness, safety boots, and safety helmet) during the experiment. Also, ironwork-related tools (*e.g.*, sleever bar, spud wrench, and dual ratchet spud) were attached on the subjects' tool belts to create a similar experience to actual ironwork. A total of nine subjects without ironwork experience walked on the 0.15-meter-wide steel I-beam surface with their typical walking speed. The detail of subject information is shown in Table 1.

This study conducted five different experiments to study the feasibility of using gait abnormality for hazard identification (see Fig. 1a). First of all, subjects participated in the experiment without any hazards on the beam to collect data about each subject's normal gait patterns. Then, either the obstacle or the slippery surface was installed on the beam, and each hazard was tested at two different locations (9.1 m or 15.2 m). In this study, two different types of fall hazards—an obstacle and a slippery surface—were installed on the beam: A wooden block (see Fig. 1e) and liquid (oil) on a plastic sheath (see Fig. 1f) served as an obstacle and slippery surface, respectively. Also, due to the starting (1.5 m) and ending (22.9 m) locations on the beam as well as the eliminated data from each subject's first step/last step (which were not included within complete gait cycles), the total distance covered during this gait analysis came to 18.4 m.

A WIMU (Opal, APDM Inc.) (see Fig. 1c) was attached to the subject's right ankle (see Fig. 1d) for data collection. A WIMU collected the data from three axes of acceleration (m/s^2) and angular velocity (rad/s) with 128 Hz sampling rates. All of the experiments were video recorded, and the video was time synchronized with the WIMU data using the manufacturer software (Motion Studio, APDM Inc.). Using the collected video, the gait cycles under the influence of a hazard were manually classified. When a gait cycle had any overlap with the installed hazards, this study considered the data as being under a hazard's influence. With this rule, one-to-three consecutive gait cycles was labeled as gait data from hazards. In this study, all of computations were performed using the MATLAB (R2015, MATHWORKS).

3.2. Data preprocessing

In order to compute gait features, ambulatory gait analysis requires preprocessing steps such as gait events detection, coordinate alignment, gravity cancellation, and zero-velocity update. Of these considerations, gait-event detection is the first essential step to computing gait features. Since a gait is a cyclic movements of the foot [55], any consecutive gait events (*e.g.*, heel strike and toe-off) of one foot can be used to define a gait cycle (see Fig. 2a) [56]. This study defined gait cycle as a gait between consecutive heel strike points of one foot, similar to other gait analysis studies [36,37,56,57]. For gait-event detection, this study used pitch angle of the WIMU to identify heel strike and toe-off points, similar to a previous study [58] (see Fig. 2c).

When an WIMU is attached to lower body parts (*e.g.*, leg or foot) for computing gait features, coordinate alignment is necessary between the sensor's coordinate system (local axis system) and the body's coordinate system (global axis system). As shown in Fig. 2a, the axes of the sensor coordinate system (*i.e.*, the WIMU) are continually changing with leg movements. Thereby, the angle difference between the two coordinate systems—see theta in Fig. 2b—also changes. In order to compute gait features, acceleration data collected in the sensor's coordinate system by the WIMU need to be aligned with the body's coordinate system. For this coordinate alignment, this study utilized orientation data (*i.e.*, quaternion) from the WIMU (Opal, APDM), similar to a previous study [59]. The quaternion, which represents the object's orientation using a complex number ($\hat{q} = [q_r, q_i, q_j, q_k]^T$), is computed by performing the integration of the WIMU signals using a Kalman filter. The rotation matrix, RM, is computed using these quaternion data with following equation:

$$\mathrm{RM} = \begin{bmatrix} 1 - 2q_j^2 - 2q_k^2 & 2(q_i q_j - q_k q_r) & 2(q_i q_k + q_j q_r) \\ 2(q_i q_j - q_k q_r) & 1 - 2q_i^2 - 2q_k^2 & 2(q_j q_k - q_i q_r) \\ 2(q_i q_k - q_j q_r) & 2(q_j q_k - q_i q_k) & 1 - 2q_i^2 - 2q_j^2 \end{bmatrix} \quad (1)$$

Then, horizontal acceleration (A_h in Fig. 2b) and vertical acceleration (A_v in Fig. 2b) are computed using a rotation matrix from Eq. 1 and acceleration data from the WIMU (A_x, A_y, and A_z). Also, vertical acceleration (A_v) offsets the influence of gravity (approximately 9.81 m/s^2) to enable the computation of vertical movement-related gait features (*i.e.*, maximum foot clearance). Details of the computation

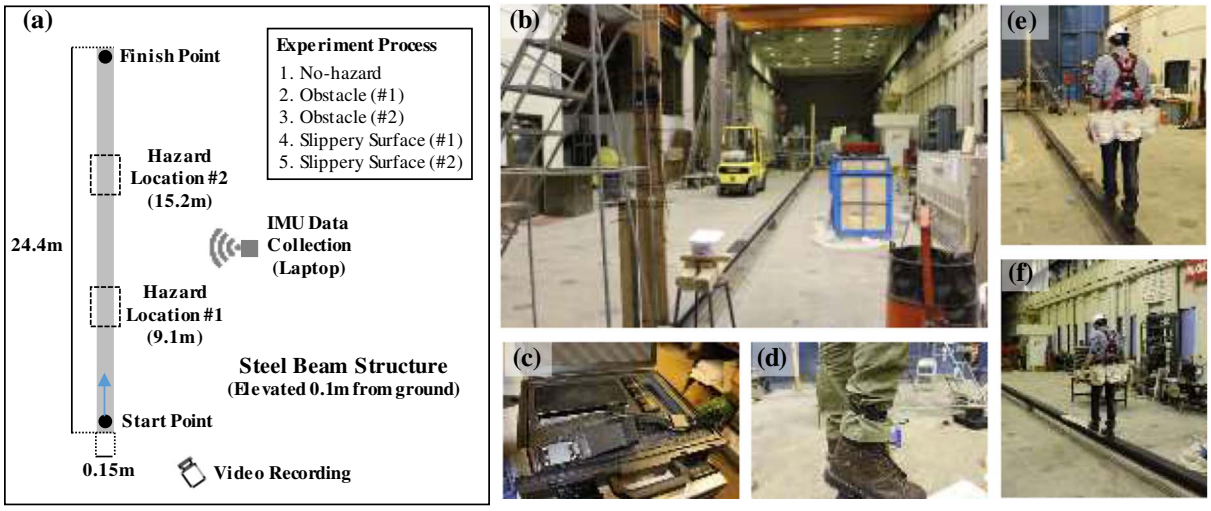

Fig. 1. Laboratory experiment setups: (a) experiment overview; (b) laboratory experiment settings; (c) WIMU System (Opal, APDM Inc.); (d) WIMU installation for gait kinematic data collection; (e) obstacle on the steel beam structure; and (f) slippery surface on the steel beam structure.

Table 1
Detailed information about experiment subjects.

	Height (cm)	Weight (kg)	Shoe size (U.S.)	Age (years)
Mean	177.22	75.89	9.56	27.56
Median	178.00	76.00	9.78	27.78
Min	165.00	60.00	7.00	25.00
Max	187.00	88.00	12.00	30.00
Standard deviation	6.68	8.33	1.42	1.42

processes follow this equation:

$$\begin{bmatrix} A_h \\ A_m \\ A_v \end{bmatrix} = RM \times \begin{bmatrix} A_x \\ A_y \\ A_z \end{bmatrix} + \begin{bmatrix} 0 \\ 0 \\ 9.81 \end{bmatrix} \quad (2)$$

where, A_h, A_m, and A_v are horizontal (same as anterior-posterior), mediolateral, and vertical axis accelerations in the body's coordinate system, respectively.

In this study, gait feature that are related to the mediolateral axis (*i.e.*, stride width) are not measured since the steel beam surface had a narrow width (*i.e.*, 0.15 m), causing subjects to maintain a narrow stride width while walking on the beam during the experiment. Raw IMU data and the preprocessing results are displayed in Fig. 3.

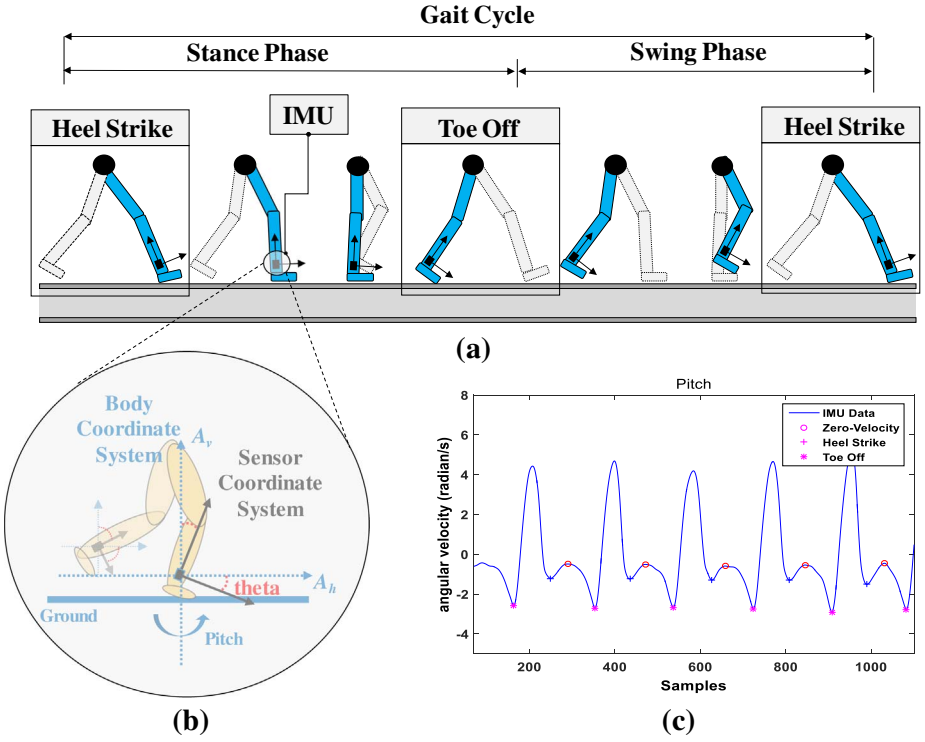

Fig. 2. (a) Definition of gait cycle; (b) sensor coordinate system and body coordinate system; (c) gait-event (zero-velocity, heel-strike, toe-off) detection with angular velocity data in anterior-posterior axis (Adapted from our previous study [53]).

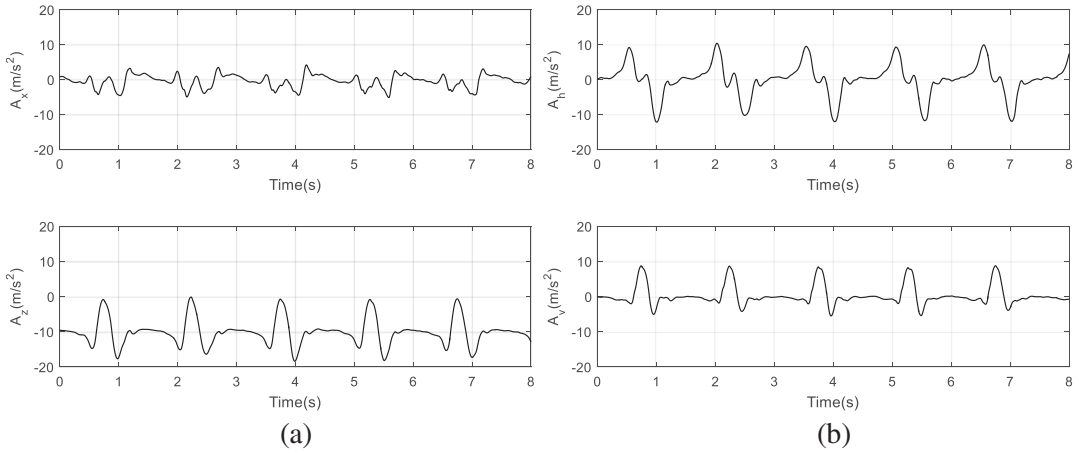

Fig. 3. (a) Raw accelerations in x- and z-axes (A_x and A_z); (b) adjusted accelerations in horizontal and vertical axes (A_h and A_v) after coordinate alignment and gravity cancellation;

Sensor drift is a well-known challenge for gait analysis [60] and IMU-based localization techniques (*e.g.*, dead reckoning) [61]. Specifically, sensor drift can cause huge errors when finding an integral of acceleration for measuring a spatially related gait feature (*e.g.*, stride distance). For example, when the foot is located on the ground during stance phase, the velocity of the WIMU has to be zero since a foot is located on the ground. However, the sensor will record a small velocity in this moment, and these errors are accumulated across gait cycles. To address this problem, this study used the widely applied zero-velocity update (ZUPT) technique, which updates zero velocity when the foot is located horizontally on the ground during stance phase (also called the "zero-velocity point"). By updating the zero for every zero-velocity point, sensor drifts or measurement errors are effectively compensated for in each gait cycle, and this technique has been shown to be reliably accurate in other gait-analysis studies [36,57,60]. In this study, the ZUPT technique was used for both horizontal and vertical velocity computation.

3.3. Gait-feature computation

This study used six available spatiotemporal gait features (stride time, stride distance, average velocity, maximum foot clearance, stance ratio, and swing ratio) expressed within the WIMU data (see Fig. 4 for details of spatiotemporal gait features from foot kinematics).

These gait features are also used in the ambulatory gait analysis with WIMU for patients and the elderly [39,61,62]. Equations for each gait feature computation are as follows:

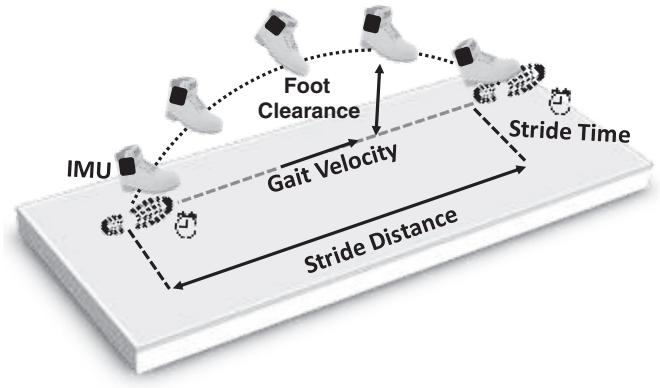

Fig. 4. Foot kinematics and spatiotemporal gait features.

(1) Stride time (*ST*), the time between heel strike events of one foot:

$$ST = t(HS_{i+1}) - t(HS_i) \tag{3}$$

where, $t(HS_{i+1})$ is the time of the $(i+1)^{th}$ heel strike event and $t(HS_i)$ is the time of the i^{th} heel strike event.

(2) Stride distance (*SD*), the traveling distance during a gait cycle:

$$SD = \int_{t(HS_i)}^{t(HS_{i+1})} V_h(t)dt \tag{4}$$

where, V_h is the horizontal velocity during the gait at time *t*.

(3) Average velocity ($\overline{V_h}$,) the average of horizontal velocity during a gait cycle:

$$\overline{V_h} = \frac{1}{t(HS_{i+1}) - t(HS_i)} \int_{t(HS_i)}^{t(HS_{i+1})} V_h(t)dt \tag{5}$$

(4) Maximum foot clearance (*MaxFC*), the maximum foot height from the ground during a gait cycle:

$$MaxFC = \max_{t\in\{t(HS_i),\cdots,t(HS_{i+1})\}} FC(t) \tag{6}$$

where FC(t) is the foot height from the ground (*i.e.*, integral of the vertical velocity).

(5) Stance ratio (*StR*), the ratio of stance phase time to gait cycle time:

$$StR = \frac{t(TO_i) - t(HS_i)}{t(HS_{i+1}) - t(HS_i)} \tag{7}$$

where $t(TO_i)$is the time of i^{th} toe-off event.

(6) Swing ratio (*SwR*), the ratio of swing-phase time to gait-cycle time:

$$SwR = \frac{t(HS_{i+1}) - t(TO_i)}{t(HS_{i+1}) - t(HS_i)} \tag{8}$$

In this study, the WIMU data from the start point in Fig. 1a to first heel strike point and from last heel strike point to the finish point in Fig. 1a of each trial are neglected in the gait-feature computation; these events are not contained within the entire cycle. The computed gait features are used to measure the degree of gait disruption through a gait-abnormality measurement technique.

The validity of the gait-feature computations presented here was also tested using additional experiments. Specifically, this study compared two gait features (stride time and stride distance) as computed from WIMU data with ground truth data that were manually collected using a ruler and a timer. In this validating study, a WIMU sensor was

attached to the subject's right ankle, and the subject walked on the laboratory floor without the interference of a hazard. The experiment organizer collected a total of 45 samples of stride time and stride distance data manually. Then, the manually collected data were compared with the stride time and stride distance computed from the WIMU data using root mean square error (RMSE). The computed stride time and stride distance were within 0.23 s RMSE and 0.09 m RMSE of the reference data, respectively, which equates to less than 10% of the average stride time (3.984 s) and stride distance (1.216 m). This study also conducted a paired-sample *t*-test and confirmed that the computed stride distance and stride time did not have a significant difference ($p > 0.05$) when compared to the reference data.

3.4. Gait abnormality measurement

Approaches to using a single score to represent the degree of a gait's deviation have been studied in clinical applications. The most widely used approaches are the Gillette Gait Index (GGI) [31,58,63] and the Gait Deviation Index (GDI) [32,64]. These approaches measure the distance of multiple gait features between healthy subjects and Parkinson's or Cerebral Palsy patients in the principal component space. Such approaches effectively quantify the deviation of gait features between patients and healthy subjects. However, these metrics have not been used to quantify the gait disruption of a single subject (called the subject's gait abnormality) when meeting hazards during a gait. Furthermore, these existing metrics require multiple joint-angle data (16 angles of joints) for computation; data requirements create challenges to applying the existing approaches to measuring the deviation of gait features in a construction environment.

Given the need for a gait abnormality measuring technique for the construction environment, this study proposes an IMU-based Gait Abnormality Score, which measures the deviations of a single subject's momentary stride from a distribution of his/her normal strides. This study used the Mahalanobis distance (MD) metric, which can measure the distance between a given sample point and a group of reference data while considering the distribution of the reference data as a whole [67]. The MD metric is widely used to solve clustering problems and to detect outliers in multivariate analysis [18,65]. Specifically, the inverse covariance matrix (C^{-1} in Eq. 9, below) makes each feature have same degree of dispersion when measuring a distance using the MD metric. Thereby, the MD metric rescales each dimension to have a unit variance to measure the distance between the sample point and the center of the distribution and the proposed I-GAS handles the correlation and measurement unit difference between gait features. Consequently, the proposed I-GAS quantifies the changes within an individual's gait features—collected *via* the WIMU—by comparing the changes with his/her gait features in non-hazard conditions. Eq. 9 is as follows:

$$I - GAS_i = \sqrt{(x_i - \overline{y})^T C^{-1} (x_i - \overline{y})} \quad (9)$$

where, x is a (1 × M) vector of gait features (M) from ith gait cycle, $\overline{y}$ is a (1 × M) mean vector of gait features (M) from reference data (y), and C^{-1} is an inverse covariance matrix of reference data (y).

4. Gait feature computation result

4.1. Data overview

After executing the preprocessing steps described above, the study computed both the horizontal and vertical velocities. The computed velocities data showed changes in the subjects' gait patterns when interacting with a hazard as compared to the gait patterns without hazards (see Fig. 5). With the obstacle, both the horizontal and vertical velocities showed decrease patterns at the hazardous location. On the other hand, the slippery surface show a smaller difference compared to the obstacle, but the length of the subjects' gait-cycle time decreased as compared to the non-hazardous conditions. The preprocessed IMU data showed the existence of a gait disruption in the hazardous locations, and this study computed the gait features to effectively measure such gait disruptions quantitatively.

4.2. Gait feature computation result

This study analyzed the gait features for both hazardous and non-hazardous cases. The results of the gait-feature computation revealed the existence of gait disruptions in both types of hazardous cases, and these gait disruptions were observed in all subjects (see Table 2).

With the obstacle hazard, most of the subjects, except one subject, decreased their gait velocity (*i.e.*, average velocity) and had longer stride times. The stride distance and swing ratio also decreased 6.2% and 10.5%, respectively, as compared to the subjects' normal gaits. On the other hand, the maximum foot clearance increased substantially (at least 10%) to avoid the obstacle. Lastly, the swing ratio increased 8.5% when encountering the obstacle hazard.

With the slippery surface hazard, subjects also decreased their gait speed and had longer stride times, similar to the obstacle. Subjects' stride distances decreased more than 10% to respond the slippery hazard. The maximum foot height and swing ratio decreased 3.4% and 9.6% when confronted with the slippery surface, while the stance ratio increased 7.5%.

Among the gait features, the maximum foot clearance shows the biggest difference (*i.e.*, 35%) between the two hazards because of the different mechanisms involved in inducing a fall. For example, an obstacle makes a subject increase her maximum/minimum foot height to avoid a tripping accident whereas a slippery surface makes a subject decrease her foot height to have more time during a gait. The corresponding characteristics of a hazard therefore yield different maximum foot heights depending on the type of hazard, which presents an opportunity for identifying the type of hazard using certain gait features.

Although the gait analysis results show the existence of gait disruptions by hazards, each subject has an individual difference in his gait responses. In Fig. 6, Subject #1 and Subject #2 have different response patterns to the same hazard. For example, for Subject #1, the stride time increases substantially at both hazards, while Subject #2 has comparably smaller increases. Also, Subject #2 has similar changes in stance ratio and swing ratio from both hazards, whereas Subject #1 does not. In addition, each subject has a different sensitivity to differentiating a hazard even when using the same gait feature.

These outcomes are important to applications in construction since various types of fall hazards exist on a construction site and current knowledge cannot determine which gait features are sensitive enough to identify such hazards. These findings do support the use of the I-GAS for measuring the abnormality of multiple gait features at a time.

5. Hazard identification with I-GAS

Using the Mahalanobis distance metric, each subject's gait disruptions were measured *via* a single score that represented the degree of the gait disruption the subject experienced in response to the hazards. The I-GAS results demonstrate a significant difference (two-sample *t*-test, $p < 0.01$) between both hazardous cases and the non-hazardous case. Installed hazards generated higher I-GAS values (*i.e.*, higher degrees of gait disruption) compared to the non-hazardous conditions. Specifically, the obstacle had a higher I-GAS value (14.974) compared to the slippery surface (12.456), and the non-hazardous condition had a comparably lower I-GAS compared to both hazardous cases (see Fig. 7). This result shows that the proposed gait-abnormality approach can capture gait disruptions in hazardous conditions and that the I-GAS can represent the degree of gait disruption with a single score.

On the other hand, even in a laboratory setting, some experiment subjects modified their gait patterns (*e.g.*, changed their gait speeds) at the non-hazardous locations, which linked these changes to high I-GAS

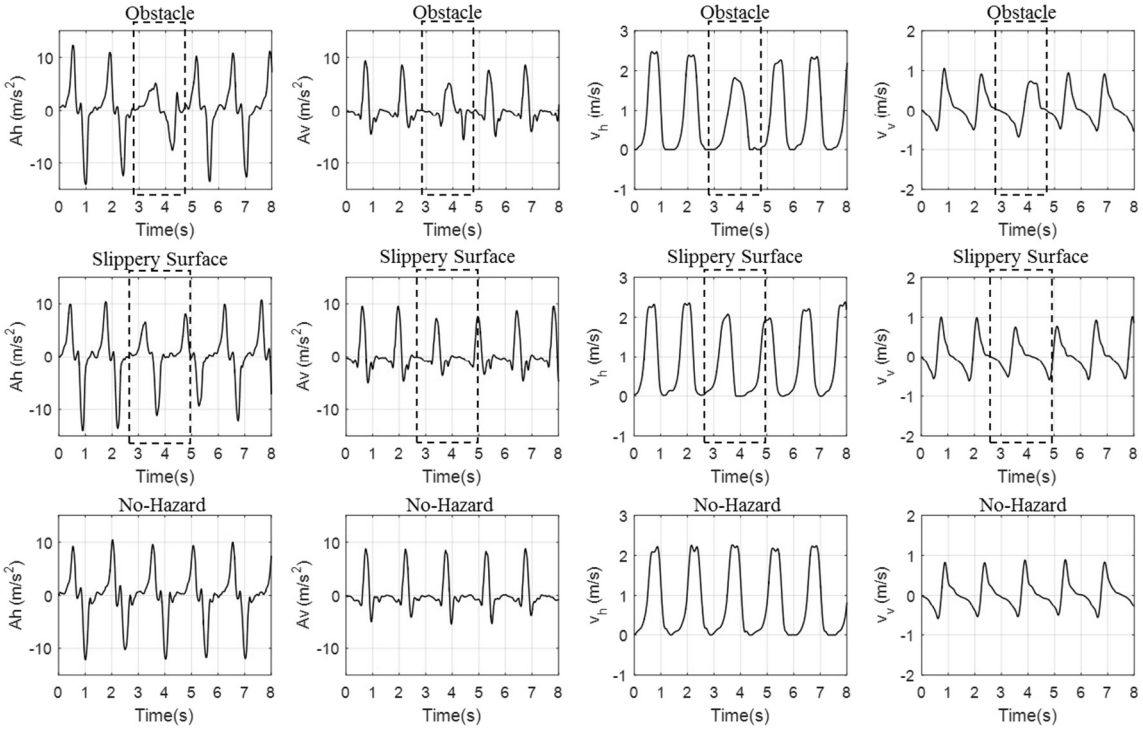

Fig. 5. Changes in horizontal acceleration (A_h), vertical acceleration (A_v), horizontal velocity (V_h), and vertical velocity (V_v) in obstacle, slippery surface, and non-hazardous locations.

values (see Fig. 8). The high I-GAS outcomes from the non-hazardous locations can decrease the hazard-identification performance substantially, especially in actual construction site. Considering the fact that a construction environment has a higher probability of prompting irrelevant gait-pattern changes in non-hazardous locations, further analysis of these outcomes becomes necessary to address this limitation for actual implementation in the construction site.

To address this limitation, this study aggregated the I-GAS data of multiple workers based on their collected locations (*i.e.*, collective sensing) to focus on the spatial pattern of subjects' responses. This study deemed this aggregated I-GAS as Local I-GAS (see Eq. 10). With this approach, all of the irrelevant I-GAS peaks in non-hazardous locations are successfully filtered out, and only hazardous locations appear as peaks. Thus, this aggregated approach can improve the identification performance compared to raw I-GAS results.

$$\text{Local I-GAS}_i = \frac{1}{n}\sum_{j=1}^{n} \text{I-GAS}_{ij} \tag{10}$$

where I-GAS_i is the collected I-GAS at the location i, and n is the total number of collected I-GAS in location i.

In this study, the location of each gait cycle was determined based on the stride distance of each gait cycle. This technique is similar to the IMU-based location technique (*i.e.*, Pedestrian Dead-Reckoning) in previous studies, and it shows reliable accuracy in total traveling-distance estimation [62,68,69]. Also, distance errors between total covered distance and total stride distance can be equally distributed to each gait cycle. As this study defined the gait cycle as the gait between consecutive right heel strikes, the total covered distance during the experiment is the distance between the first heel strike point and the last heel strike point. As a result, the spatial information of each I-GAS is assigned for aggregation. This study named each data sample from subjects as a "trial" and plotted each trial based on its locations.

Figs. 9a and 10a illustrate the spatial pattern of assigned I-GAS from all subjects. The I-GAS results show a concentration of high values at hazard locations. In detail, the obstacle has fewer unrelated peak points at the non-hazardous locations when compared to the slippery surface. These unrelated peak points are located sparsely throughout the locations, a characteristic that led this study to use the aggregation method to filter out the unrelated peak I-GAS. With data aggregation, these unrelated peak points in non-hazardous locations are successfully addressed, and only hazard locations result in a high I-GAS value. Figs. 9b and 10b present the final results from aggregating the data of all subjects encountering an obstacle and slippery surface, respectively.

This study also tested the impact of the size of the data set in aggregating I-GAS values for identifying hazards. Fig. 11 illustrates the range of mean I-GAS values from all the possible combinations by increasing the number of subjects. For example, "1 subject" in Fig. 11-a shows the distribution of aggregated I-GAS mean values from one out of all the nine subjects. Then, "2 subjects" in Fig. 11a represents the average of aggregated I-GAS values from all the possible selections of two subjects (*e.g.*, Subject 1 and 2, Subject 2 and 3). Any overlaps of the boxplots between obstacle and no-hazard indicate a possible false alarm in identifying hazards using I-GAS values. The results revealed that increasing the number of subjects is highly effective in reducing false alarms and that slippery surfaces require more data aggregation compared to obstacles in order to avoid false alarms.

To verify the performance of hazard identification using the I-GAS measurements in a quantifiable manner, this study conducted the point-biserial correlation analysis between aggregated Local I-GAS results of each location and ground truth on the hazard locations. To test the minimum and maximum performance when using data from multiple subjects, this study aggregated multiple subjects' I-GAS outcomes from the data having the lowest correlation coefficient to the data having the highest correlation coefficient. The results of this correlation analysis are presented in Table 3. Of particular note is the fact that the correlation coefficient for the obstacle increases faster than for the slippery surface; the worst scenario in our data samples—the obstacle—needed data from 4 subjects (36 trials) to have a strong correlation ($r > 0.7$) with I-GAS, whereas the slippery surface required data from 6 subjects (54 trials). These observations reveal the intensity of the magnitude of subjects' responses to obstacles as compared to slippery surfaces. In the best scenario, one subject's data was sufficient to demonstrate the strong correlation with Local I-GAS data and hazard locations. This

Table 2
Average of difference in gait features compared to the non-hazardous condition.

Subject #	Stride time	Stride distance		Maximum foot clearance		Average velocity		Stance ratio		Swing ratio	
	Obstacle (%)	Slippery surface (%)	Obstacle (%)	Slippery surface (%)	Obstacle (%)	Slippery surface (%)	Obstacle (%)	Slippery surface (%)	Obstacle (%)	Slippery surface (%)	Obstacle (%)	Slippery surface (%)
1	25.6	16.9	−2.9	0.2	22.1	9.2	−21.2	−13.4	4.7	−0.3	−5.9	0.4
2	19.9	7.6	−3.4	−20.7	25.9	−7.6	−18.2	−20.8	7.9	10.8	−8.7	−12.0
3	37.5	21.7	−8.7	−26.8	50.5	−17.0	−30.2	−31.5	15.4	9.9	−17.8	−11.5
4	1.4	11.2	−17.7	−20.4	10.9	−1.0	−13.4	−22.9	1.0	4.3	−1.2	−5.2
5	14.6	4.9	6.3	−5.3	41.0	5.1	−7.6	−7.3	9.5	−1.0	−10.3	1.1
6	35.7	31.6	−8.5	−5.8	12.2	−6.9	−27.1	−26.3	16.1	10.5	−20.9	−13.6
7	35.0	59.2	−1.7	9.2	58.3	−4.3	−24.9	−48.7	17.1	25.0	−24.4	−35.6
8	7.7	16.1	2.7	−9.8	28.3	−0.2	−5.2	−17.7	−1.9	5.2	2.1	−5.8
9	17.7	15.6	−21.6	−18.3	34.9	−7.8	−27.4	−24.1	6.3	3.5	−7.5	−4.3
Mean ± Std	21.7 ± 12.1	20.5 ± 15.5	−6.2 ± 8.5	−10.9 ± 11	31.6 ± 15.3	−3.4 ± 7.3	−17.2 ± 10.2	−23.6 ± 11.1	8.5 ± 6.4	7.5 ± 7.4	−10.5 ± 8.4	−9.6 ± 10.4

finding points to an opportunity to demonstrate that with a sufficient number of data samples, latent hazards that are otherwise challenging to detect could be identified through the proposed I-GAS approach.

6. Discussion

6.1. Performance of I-GAS-based hazard identification

This study proposes a gait abnormality measurement technique that quantifies the magnitude of disruption of a subject's gait to identify fall hazards on a surface. The results of this study confirmed that the presence of fall hazards on a surface generate disruptions in a subject's gait patterns and that these disruptions can be quantified using the proposed I-GAS. This study tested identifying two different types of common fall hazards on construction sites (an obstacle and a slippery surface). Our results show that the proposed gait abnormality measurement technique manifested a strong correlation with the tested hazards. It should be noted that this study only examined the correlation of I-GAS with the exact location of hazards, but the research team observed that a hazard prompts gait-pattern changes before/after the experience of the hazard and such high I-GAS values before/after the hazard negatively impact the correlation analysis result. However, if we can extend the correlation analysis to cover these before/after gait-response areas, the identification performance of this methodology would foreseeably increase significantly.

6.2. Relationship between spatiotemporal gait feature and fall accident

The results of the spatiotemporal gait-features analysis in this study show similar results with previous fall-risk assessment studies that use gait analysis. Jefferey [70] studied the gait variability and fall-accident experiences of older adults and found that stride-time variability highly correlates with fall-accident experience; similarly, the computed gait-feature results about stride time in this study identify stride time as showcasing one of the highest variabilities in both types of hazards. Sterke [71] predicted short-term fall risks among nursing home residents with dementia and revealed that reduced gait velocity and reduced stride length are the best predictors of fall accidents. Also, Garman [72] estimated the probability of tripping accidents from an obstacle by using a subject's gait speed and other information (*e.g.*, the height of the obstacle, age, obesity) and showed these data could assist in estimating a tripping accident.

Similar to these studies, the result of our study show that stride time and gait velocity decrease in hazard locations. These concurring outcomes reveal an opportunity to evaluate worker's gait responses to hazardous conditions in light of existing knowledge about gait analysis; by allowing these two arenas of gait analysis to work in dialogue, we may deepen our understanding and knowledge about workers' gait responses and thereby increase the opportunities for measuring each worker's risk of fall accidents, as clinical disciplines have been attempting to do. Thus, the benefits of studying human-response patterns in high fall-risk areas to identify both fall hazards and fall-prone workers continues to be a promising arena of research.

6.3. Potential applications

The proposed approach is envisioned to significantly increase hazard-identification performance on construction jobsites by providing supportive tools that add workers' gait-response data to the current safety-hazard identification efforts. For example, current identification approaches ask safety managers to conduct visual inspections, which are limited in the face of the dynamic changes taking place within a construction work environment. Also, concentrations of multiple workers' gait abnormalities can be used as immediate indicators of increasing fall-accident risks, even in changing work environments. With these data, a safety manager can decide whether to pursue additional

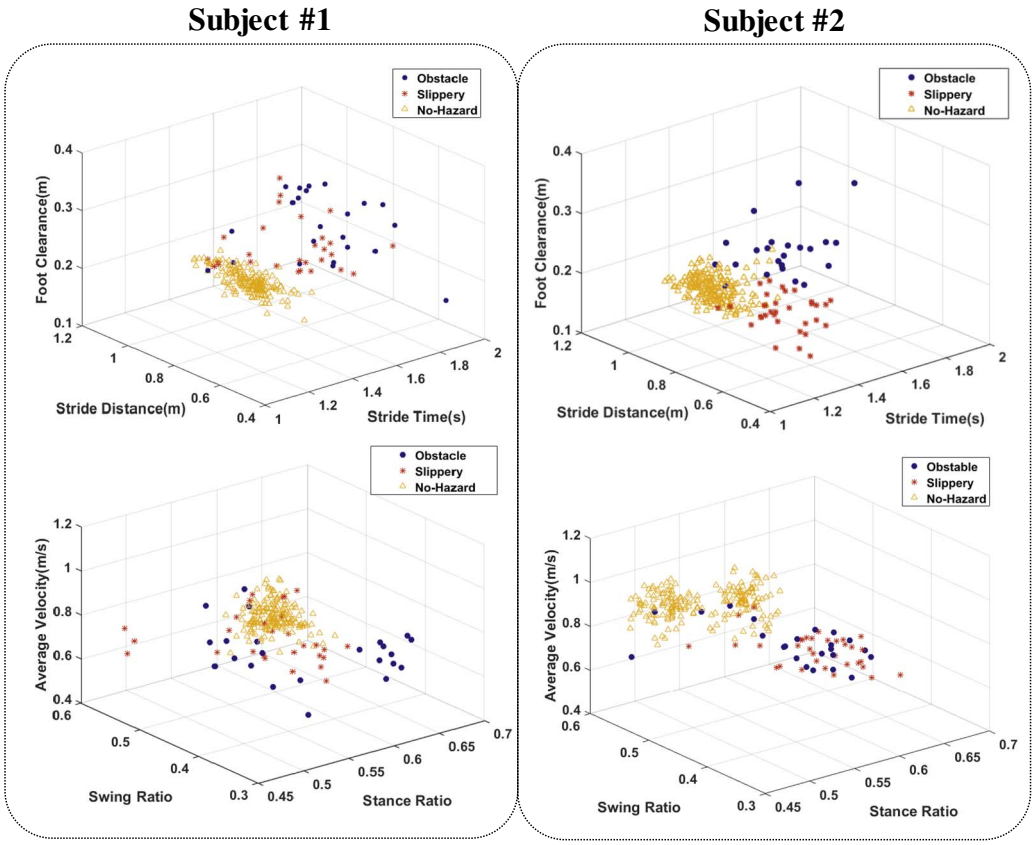

Fig. 6. Two individual subjects' gait-feature data from the obstacle, slippery surface, and no-hazard locations.

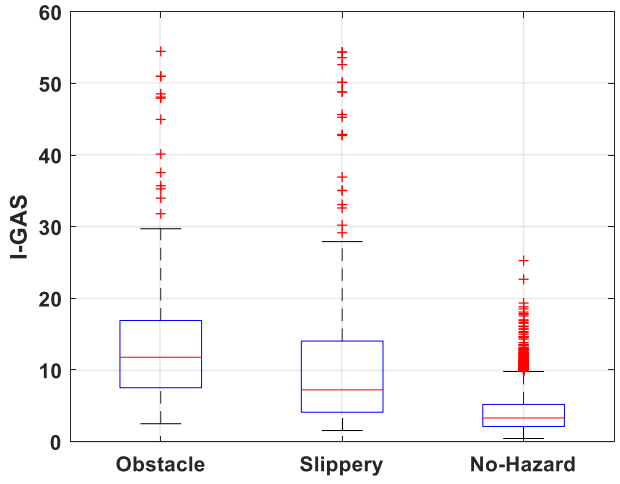

Fig. 7. Result of I-GAS computation for all subjects with obstacle, slippery surface, and no-hazard conditions.

inspection plans in the specific high-risk area. Also, the difference between the gait abnormality results and the manual inspection outcomes can be used to infer the location of latent fall hazards in the job site. With such information, a safety manager could perform further examinations in such areas to identify latent fall hazards, thereby enabling safety managers to mitigate the risk of an accident catalyzed by these hazards. Also, similar with previous study from Zhang [73], measured gait abnormalities can be mapped in the Building Information Modeling (BIM) of a construction site to assist in a safety manager's further examinations by delivering better understanding on the contexts of why gait abnormalities occur at a certain location (*e.g.*, recognized hazards, latent hazards, non-hazardous site conditions). In particular, the integration with the BIM model will help filtering out gait abnormalities caused by non-hazardous site conditions (*e.g.*, site geometry, stairs). Moreover, such the integration will facilitate the better communication among safety managers and workers on identified hazards, thereby efficiently mitigating the risks of identified hazards.

6.4. Limitations and future directions

Although the result of this study showed that the suggested method has a potential to indicate the existence of hazard in the controlled experiment setting, our experiments included only two types of hazards which are commonly found in the ironwork. Other types of hazards need to be further tested. For example, every items or conditions such as, tool boxes, other workers, dust, and unorganized electrical code in construction site, can cause abnormal gait which can be linked to STFs. Moreover, the conducted experiment tested only walking activity without any additional tasks (*e.g.*, carrying material, combined with other stationary tasks). Thus gait patterns and disruptions with additional tasks need to be investigated to demonstrate the feasibility of the proposed approach in a real world setting. In addition, it needs to be investigated how the diverse characteristics of construction workers (*e.g.*, work experience, age, gender) affect their gait responses in related to hazards.

Furthermore, the following aspects of the proposed method need to be further investigated to ensure its performance in practice. First of all, this approach requires multiple data samples to have accurate hazard identification results; unfortunately, the extended data requirement makes real-time monitoring challenging since multiple observations may take time to garner. One available approach to decreasing the data requirement is to consider additional gait features from the WIMU in the gait-abnormality measurement technique. By introducing foot angle- or foot trajectory-related features to the gait-abnormality

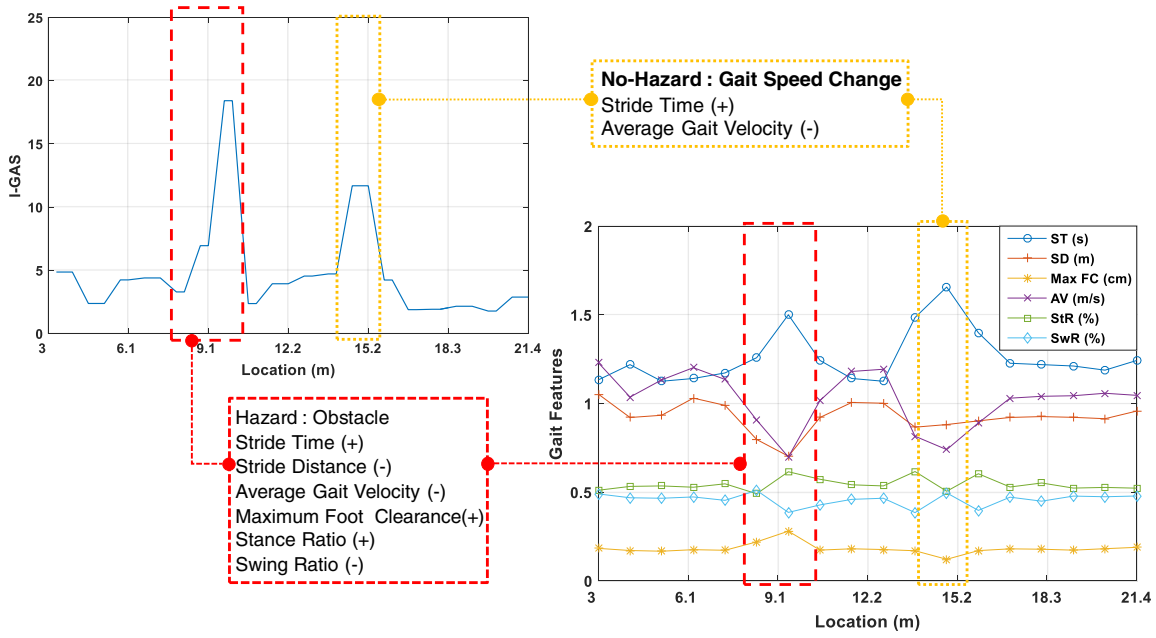

Fig. 8. High I-GAS result from non-hazardous condition.

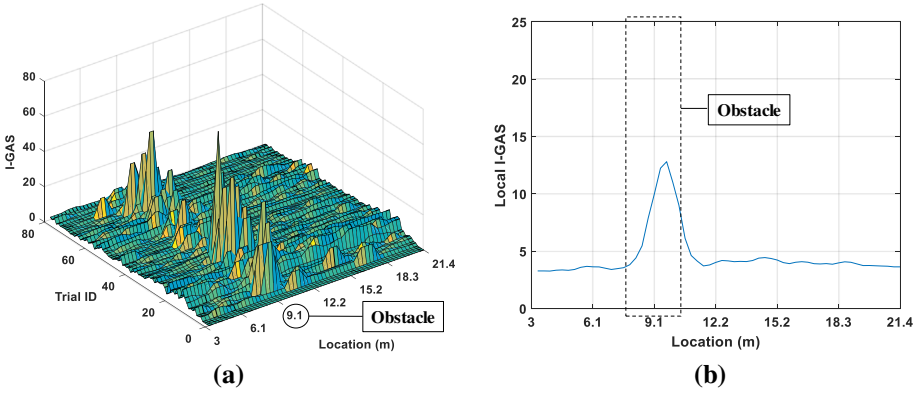

Fig. 9. I-GAS computation results: (a) spatial pattern of I-GAS with obstacle at 9.1 m; (b) Local I-GAS with obstacle at 9.1 m.

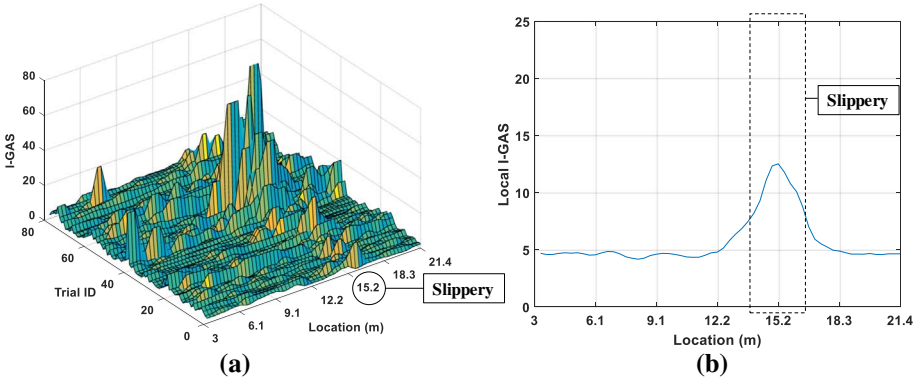

Fig. 10. I-GAS computation results: (a) spatial pattern of I-GAS with slippery surface at 15.2 m; and (b) Local I-GAS with slippery surface at 15.2 m.

measurements, deviations within workers' gait data may be more readily visible for hazard identification. Another aspect is that the proposed approach requires robust localization techniques to collect, aggregate, and link I-GAS data with hazard locations. In this study's experiment setup, the IMU-based Pedestrian Dead-Reckoning (PDR) technique can be used due to subjects' one-dimensional movement during the experiment (walk on the straight steel beam). However, the PDR technique would likely have low accuracy in real work scenarios since we would not know the trajectory of the worker or any locational information. To counter this limitation, accurate worker-location sensing becomes necessary. Considering that a subject's gait cycle usually covers between 0.8 and 1.5 m, the accuracy localization technique—-which can have an error range bellowed than worker stride distance —needs to be tested and used on a real construction site to determine

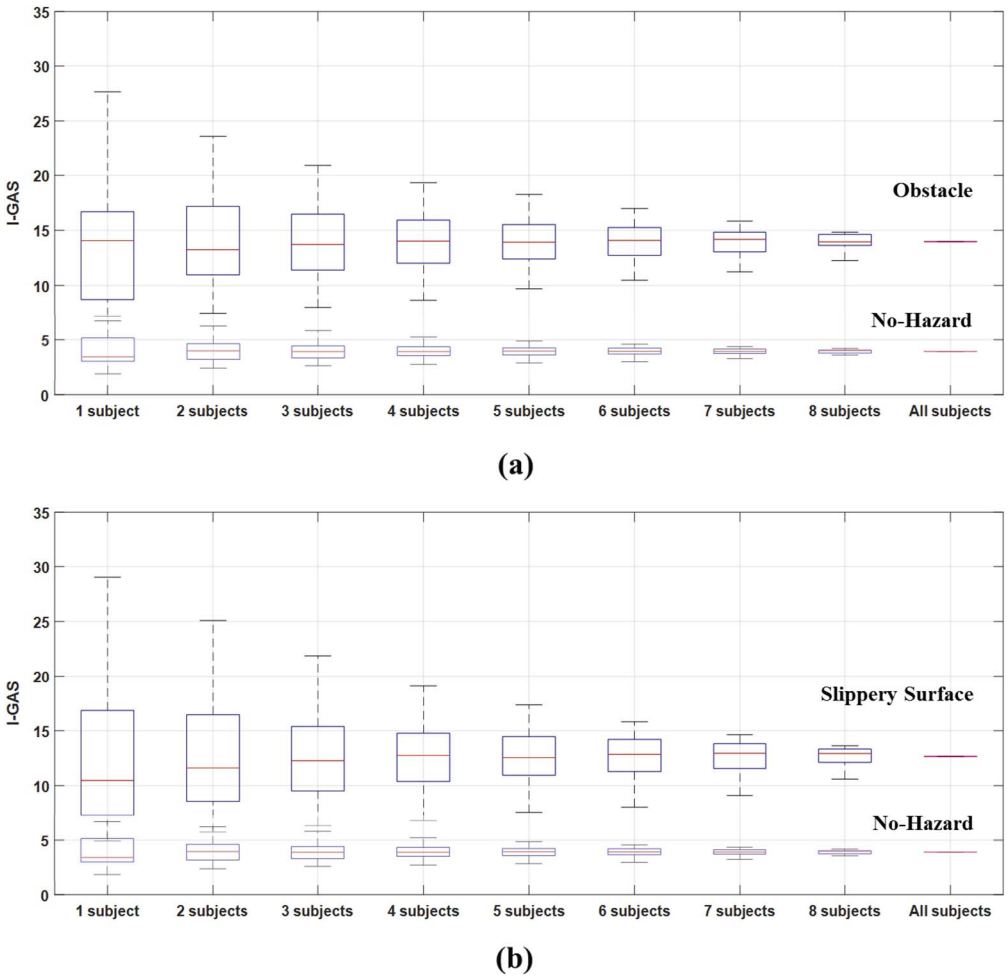

Fig. 11. Changes in I-GAS value cause by increasing the number of aggregated subjects: (a) obstacle (9.1 m), (b) slippery surface (15.2 m)

Table 3
Correlation analysis results between Local I-GAS and hazard locations.

Number of aggregated subjects	Obstacle		Slippery surface	
	Correlation coefficient (minimum)	Correlation coefficient (maximum)	Correlation coefficient (minimum)	Correlation coefficient (maximum)
1	0.3792*	0.9225*	0.2295*	0.8435*
2	0.5734*	0.9242*	0.2799*	0.8560*
3	0.6592*	0.9022*	0.3959*	0.8306*
4	0.8084*	0.9009*	0.5791*	0.8290*
5	0.8240*	0.8944*	0.6619*	0.8203*
6	0.8375*	0.9012*	0.7173*	0.8302*
7	0.8436*	0.8982*	0.7953*	0.8329*
8	0.8512*	0.8920*	0.7999*	0.8299*
9	0.8872*	0.8872*	0.8349*	0.8349*

* denotes a strong correlation ($r > 0.7$).

whether workers can be located accurately enough to make this approach viable outside the laboratory.

7. Conclusion

This study proposes a gait abnormality measurement approach to identify the existence of fall hazards on the surface of a construction environment. This study tested the proposed approach in a laboratory setting by installing an obstacle and a slippery surface as fall hazards on an I-beam. The results of the collective gait abnormality approach show a strong correlation between the location of hazards and the test subjects' physical responses to the hazards, which in turn reveal the feasibility of identifying fall hazards by measuring workers' gait disruption patterns. The results of this study will enhance safety managers' hazard-identification capabilities for detecting existing fall hazards and will help these managers eliminate these hazards on the construction site. The findings of this study can serve as a basis for developing an automated hazard-identification system that utilizes workers' physical response patterns as an informative source of data for hazard identification in construction.

As a future research direction, field experiments that include workers' natural movements and/or the various latent hazards found in real-world settings are necessary to examine the actual performance of this hazard identification methodology. Also, different types of gait disruptions—such as gait-path changes and leg-angle changes—need to be studied to capture more information from fall hazards and thereby make this approach more robust. Lastly, further explorations into locating workers need to be executed in order to identify hazard locations on two-dimensional work surfaces.

Acknowledgement

The authors would like to acknowledge Dr. Terry Stentz—Associate Professor, Durham School of Architectural Engineering and Construction, UNL—for designing and conducting the experiment and Cory Lyons—Project Manager, Davis Erection Co Inc. (Topping Out Inc.) of Lincoln, NE—for his support and technical assistance. This study was financially supported by National Science Foundation (CMMI #1538029 and CNS #1423379). Any opinions, findings, conclusions, or

recommendations expressed in this article are those of the authors and do not necessarily reflect the views of the National Science Foundation.

References

[1] M.J. Skibniewski, Information technology applications in construction safety assurance, J. Civ. Eng. Manag. 20 (2014) 778–794 https://doi.org/10.3846/13923730.2014.987693.

[2] U.C. Gatti, S. Schneider, G.C. Migliaccio, Physiological condition monitoring of construction workers, Autom. Constr. 44 (2014) 227–233 https://doi.org/10.1016/j.autcon.2014.04.013.

[3] T. Cheng, G. Migliaccio, J. Teizer, U. Gatti, Data fusion of real-time location sensing and physiological status monitoring for ergonomics analysis of construction workers, J. Comput. Civ. Eng. 27 (2013) 320–335 https://doi.org/10.1061/(ASCE)CP.1943-5487.0000222.

[4] P. Mitropoulos, T. Abdelhamid, G. Howell, Systems model of construction accident causation, J. Constr. Eng. Manag. 131 (2005) 816–825 https://doi.org/10.1061/(ASCE)0733-9364(2005)131:7(816.

[5] H.J. Lipscomb, J.E. Glazner, J. Bondy, K. Guarini, D. Lezotte, Injuries from slips and trips in construction, Appl. Ergon. 37 (2006) 267–274 https://doi.org/10.1016/j.apergo.2005.07.008.

[6] A. Albert, M.R. Hallowell, B. Kleiner, A. Chen, M. Golparvar-Fard, Enhancing construction hazard recognition with high-fidelity augmented virtuality, J. Constr. Eng. Manag. 140 (2014) 4014024 https://doi.org/10.1061/(ASCE)CO.1943-7862.0000860.

[7] G. Carter, S. Smith, Safety hazard identification on construction projects, J. Constr. Eng. Manag. 132 (2006) 197–205 https://doi.org/10.1061/(ASCE)0733-9364(2006)132:2(197.

[8] K. Kemmlert, L. Lundholm, Slips, trips and falls in different work groups—with reference to age and from a preventive perspective, Appl. Ergon. 32 (2001) 149–153 https://doi.org/10.1016/S0003-6870(00)00051-X.

[9] H.-Y. Yoon, T.E. Lockhart, Nonfatal occupational injuries associated with slips and falls in the United States, Int. J. Ind. Ergon. 36 (2006) 83–92 https://doi.org/10.1016/j.ergon.2005.08.005.

[10] H.T. Yeoh, T.E. Lockhart, X. Wu, Non-fatal occupational falls on the same level, Ergonomics 56 (2013) 153–165 https://doi.org/10.1080/00140139.2012.746739.

[11] A.K. Bourke, J.V. O'Brien, G.M. Lyons, Evaluation of a threshold-based tri-axial accelerometer fall detection algorithm, Gait Posture 26 (2007) 194–199 https://doi.org/10.1016/j.gaitpost.2006.09.012.

[12] A.K. Bourke, G.M. Lyons, A threshold-based fall-detection algorithm using a bi-axial gyroscope sensor, Med. Eng. Phys. 30 (2008) 84–90 https://doi.org/10.1016/j.medengphy.2006.12.001.

[13] C.-F. Lai, S.-Y. Chang, H.-C. Chao, Y.-M. Huang, Detection of cognitive injured body region using multiple triaxial accelerometers for elderly falling, IEEE Sensors J. 11 (2011) 763–770 https://doi.org/10.1109/JSEN.2010.2062501.

[14] T.-K. Lim, S.-M. Park, H.-C. Lee, D.-E. Lee, Artificial neural network–based slip-trip classifier using smart sensor for construction workplace, J. Constr. Eng. Manag. 142 (2016) 4015065 https://doi.org/10.1061/(ASCE)CO.1943-7862.0001049.

[15] R.-J. Dzeng, Y.-C. Fang, I.-C. Chen, A feasibility study of using smartphone built-in accelerometers to detect fall portents, Autom. Constr. 38 (2014) 74–86 https://doi.org/10.1016/j.autcon.2013.11.004.

[16] I. Altman, J.F. Wohlwill, Human Behavior and Environment: Advances in Theory and Research, Springer Science & Business Media, 2012 ISBN 978-1-4684-0810-2.

[17] R. Gifford, Environmental Psychology: Principles and Practice, Optimal books Colville, WA, 978-0993771903, 2007.

[18] S. Xiang, F. Nie, C. Zhang, Learning a Mahalanobis distance metric for data clustering and classification, Pattern Recogn. 41 (2008) 3600–3612 https://doi.org/10.1016/j.patcog.2008.05.018.

[19] U.S. Bureau of Labor Statistics, Census of Fatal Occupational Injuries - Current and Revised Data, 2015 (Available on-line via http://www.bls.gov/iif/oshcfoi1.htm) (Accessed Mar 2017).

[20] T.K. Courtney, S. Matz, B.S. Webster, Disabling occupational injury in the US construction industry, 1996, J. Occup. Environ. Med. 44 (2002) 1161–1168 (ISSN: 1076-2752 (PMID: 12500458)).

[21] G.H. Cattledge, A. Schneiderman, R. Stanevich, S. Hendricks, J. Greenwood, Nonfatal occupational fall injuries in the West Virginia construction industry, Accid. Anal. Prev. 28 (1996) 655–663, http://dx.doi.org/10.1016/0001-4575(96)00026-7.

[22] X. Huang, J. Hinze, Analysis of construction worker fall accidents, J. Constr. Eng. Manag. 129 (2003) 262–271 10.1061/(ASCE)0733-9364(2003)129:3(262).

[23] C.-F. Chi, T.-C. Chang, H.-I. Ting, Accident patterns and prevention measures for fatal occupational falls in the construction industry, Appl. Ergon. 36 (2005) 391–400 10.1016/j.apergo.2004.09.011.

[24] A. Albert, M. Hallowell, B. Kleiner, Enhancing construction hazard recognition and communication with energy-based cognitive mnemonics and safety meeting maturity model: multiple baseline study, J. Constr. Eng. Manag. 140 (2014) 4013042, http://dx.doi.org/10.1061/(ASCE)CO.1943-7862.0000790.

[25] S. Bahn, Workplace hazard identification and management: the case of an underground mining operation, Saf. Sci. 57 (2013) 129–137, http://dx.doi.org/10.1016/j.ssci.2013.01.010.

[26] R. Sacks, A. Perlman, R. Barak, Construction safety training using immersive virtual reality, Constr. Manag. Econ. 31 (2013) 1005–1017, http://dx.doi.org/10.1080/01446193.2013.828844.

[27] V.V. Khanzode, J. Maiti, P.K. Ray, Occupational injury and accident research: a comprehensive review, Saf. Sci. 50 (2012) 1355–1367, http://dx.doi.org/10.1016/j.ssci.2011.12.015.

[28] L. Decker, J.J. Houser, J.M. Noble, G.M. Karst, N. Stergiou, The effects of shoe traction and obstacle height on lower extremity coordination dynamics during walking, Appl. Ergon. 40 (2009) 895–903, http://dx.doi.org/10.1016/j.apergo.2008.12.005.

[29] C. Gao, J. Abeysekera, A systems perspective of slip and fall accidents on icy and snowy surfaces, Ergonomics 47 (2004) 573–598 https://doi.org/10.1080/00140130410081658718.

[30] A. Muro-de-la-Herran, B. Garcia-Zapirain, A. Mendez-Zorrilla, Gait analysis methods: an overview of wearable and non-wearable systems, highlighting clinical applications, Sensors 14 (2014) 3362–3394, http://dx.doi.org/10.3390/s140203362.

[31] T.A. Wren, K.P. Do, R. Hara, F.J. Dorey, R.M. Kay, N.Y. Otsuka, Gillette Gait Index as a gait analysis summary measure: comparison with qualitative visual assessments of overall gait, J. Pediatr. Orthop. 27 (2007) 765–768, http://dx.doi.org/10.1097/BPO.0b013e3181558ade.

[32] G.J. Barton, M.B. Hawken, G. Holmes, M.H. Schwartz, A gait index may underestimate changes of gait: a comparison of the Movement Deviation Profile and the Gait Deviation Index, Computer Methods in Biomechanics and Biomedical Engineering. 18 (2015) 57–63, http://dx.doi.org/10.1080/10255842.2013.776549.

[33] M. Hars, F.R. Herrmann, A. Trombetti, Reliability and minimal detectable change of gait variables in community-dwelling and hospitalized older fallers, Gait Posture 38 (2013) 1010–1014, http://dx.doi.org/10.1016/j.gaitpost.2013.05.015.

[34] C. Pradhan, M. Wuehr, F. Akrami, M. Neuhaeusser, S. Huth, T. Brandt, K. Jahn, R. Schniepp, Automated classification of neurological disorders of gait using spatio-temporal gait parameters, J. Electromyogr. Kinesiol. 25 (2015) 413–422, http://dx.doi.org/10.1016/j.jelekin.2015.01.004.

[35] M.O. Derawi, Accelerometer-based gait analysis, a survey, Proceedings of Norwegian Information Security Conference, NISK (NISK 2010), 2010, pp. 33–44.

[36] S.J.M. Bamberg, A.Y. Benbasat, D.M. Scarborough, D.E. Krebs, J.A. Paradiso, Gait analysis using a shoe-integrated wireless sensor system, IEEE Trans. Inf. Technol. Biomed. 12 (2008) 413–423, http://dx.doi.org/10.1109/TITB.2007.899493.

[37] M. Chen, B. Huang, Y. Xu, Intelligent shoes for abnormal gait detection, IEEE International Conference on Robotics and Automation, 2008, pp. 2019–2024, , http://dx.doi.org/10.1109/ROBOT.2008.4543503.

[38] S.R. Hundza, W.R. Hook, C.R. Harris, S.V. Mahajan, P.A. Leslie, C.A. Spani, L.G. Spalteholz, B.J. Birch, D.T. Commandeur, N.J. Livingston, Accurate and reliable gait cycle detection in Parkinson's disease, IEEE Transactions on Neural Systems and Rehabilitation Engineering 22 (2014) 127–137, http://dx.doi.org/10.1109/TNSRE.2013.2282080.

[39] B. Mariani, C. Hoskovec, S. Rochat, C. Büla, J. Penders, K. Aminian, 3D gait assessment in young and elderly subjects using foot-worn inertial sensors, J. Biomech. 43 (2010) 2999–3006, http://dx.doi.org/10.1016/j.jbiomech.2010.07.003.

[40] F. Parisi, G. Ferrari, A. Baricich, M. D'Innocenzo, C. Cisari, A. Mauro, Accurate gait analysis in post-stroke patients using a single inertial measurement unit, IEEE 13th International Conference on Wearable and Implantable Body Sensor Networks (BSN), 2016, pp. 335–340, , http://dx.doi.org/10.1109/BSN.2016.7516284.

[41] M.R. Patterson, W. Johnston, N. O'Mahony, S. O'Mahony, E. Nolan, B. Caulfield, Validation of temporal gait metrics from three IMU locations to the gold standard force plate, 38th Annual International Conference of the IEEE Engineering in Medicine and Biology Society (EMBC), 2016, pp. 667–671, , http://dx.doi.org/10.1109/EMBC.2016.7590790.

[42] Teizer, J., O. Golovina, D. Wang, and N. Pradhanang. Automated collection, identification, localization, and analysis of worker-related proximity hazard events in heavy construction equipment operation. In ISARC. Proceedings of the 32nd International Symposium on Automation and Robotics in Construction, (2015) 1–9, (Available on-line via: http://www.iaarc.org/publications/fulltext/FFACE-ISARC15-3002351.pdf) (Accessed on March, 2017).

[43] S.-N. Min, J.-Y. Kim, M. Parnianpour, The effects of experience and the presence of a scaffold handrail on postural and spinal stability in construction workers, Int. J. Occup. Saf. Ergon. 20 (2014) 491–502, http://dx.doi.org/10.1080/10803548.2014.11077062.

[44] J. Chen, X. Song, Z. Lin, Revealing the “invisible gorilla” in construction: estimating construction safety through mental workload assessment, Autom. Constr. 63 (2016) 173–183, http://dx.doi.org/10.1016/j.autcon.2015.12.018.

[45] L. Joshua, K. Varghese, Accelerometer-based activity recognition in construction, J. Comput. Civ. Eng. 25 (2011) 370–379, http://dx.doi.org/10.1061/(ASCE)CP.1943-5487.0000097.

[46] H. Jebelli, C.R. Ahn, T.L. Stentz, Comprehensive fall-risk assessment of construction workers using inertial measurement units: validation of the gait-stability metric to assess the fall risk of iron workers, J. Comput. Civ. Eng. 30 (2016) 4015034, http://dx.doi.org/10.1061/(ASCE)CP.1943-5487.0000511.

[47] H. Jebelli, C.R. Ahn, T.L. Stentz, Fall risk analysis of construction workers using inertial measurement units: validating the usefulness of the postural stability metrics in construction, Saf. Sci. 84 (2016) 161–170, http://dx.doi.org/10.1016/j.ssci.2015.12.012.

[48] E. Valero, A. Sivanathan, F. Bosché, M. Abdel-Wahab, Musculoskeletal disorders in construction: a review and a novel system for activity tracking with body area network, Appl. Ergon. 54 (2016) 120–130, http://dx.doi.org/10.1016/j.apergo.2015.11.020.

[49] K. Yang, C.R. Ahn, M.C. Vuran, S.S. Aria, Semi-supervised near-miss fall detection for ironworkers with a wearable inertial measurement unit, Autom. Constr. 68 (2016) 194–202, http://dx.doi.org/10.1016/j.autcon.2016.04.007.

[50] K. Yang, H. Jebelli, C.R. Ahn, M.C. Vuran, Threshold-based approach to detect near-

miss falls of iron workers using inertial measurement units, 2015 International Workshop on Computing in Civil Engineering, 2015, pp. 148–155, , http://dx.doi.org/10.1061/9780784479247.019.
[51] K. Yang, S. Aria, T.L. Stentz, C.R. Ahn, Automated detection of near-miss fall incidents in iron workers using inertial measurement units, construction research congress 2014, ASCE (2014) 935–944, http://dx.doi.org/10.1061/9780784413517.096.
[52] H. Kim, C.R. Ahn, K. Yang, Identifying safety hazards using collective bodily responses of workers, J. Constr. Eng. Manag. 143 (2016) 04016090, http://dx.doi.org/10.1061/(ASCE)CO.1943-7862.0001220.
[53] K. Yang, C.R. Ahn, M.C. Vuran, H. Kim, Sensing workers gait abnormality for safety hazard identification, Proceedings of the 33rd International Symposium on Automation and Robotics in Construction, (2016), 957–965, (Available on-line via: http://www.iaarc.org/publications/fulltext/ISARC2016-Paper189.pdf) (Accessed on March, 2017).
[54] The Center for Construction Research and Training (CPWR), Fatal and Nonfatal Injuries from Falls in Construction, in: CPWR, The Construction Chart Book, CPWR, 2013, pp. 44 (Available on-line via: http://www.cpwr.com/sites/default/files/publications/CB%20page%2044.pdf) (Accessed on March, 2017).
[55] V.T. Inman, H.J. Ralston, F. Todd, Human Walking, Williams & Wilkins, 1981 ISSN: 978-0683073607.
[56] S.-W. Lee, K. Mase, K. Kogure, Detection of spatio-temporal gait parameters by using wearable motion sensors, IEEE, 2006: 6836–6839, https://doi.org/10.1109/IEMBS.2005.1616075.
[57] K. Aminian, B. Najafi, C. Büla, P.-F. Leyvraz, P. Robert, Spatio-temporal parameters of gait measured by an ambulatory system using miniature gyroscopes, J. Biomech. 35 (2002) 689–699, http://dx.doi.org/10.1016/S0021-9290(02)00008-8.
[58] A.M. Sabatini, C. Martelloni, S. Scapellato, F. Cavallo, Assessment of walking features from foot inertial sensing, IEEE Trans. Biomed. Eng. 52 (2005) 486–494, http://dx.doi.org/10.1109/TBME.2004.840727.
[59] P.J. Bertrand, A. Anderson, A. Hilbert, D.J. Newman, Feasibility of spacesuit kinematics and human-suit interactions, 44th International Conference on Environmental Systems, (2014) (Available on-line via: https://repositories.tdl.org/ttu-ir/handle/2346/59680) (accessed September, 2016).
[60] S. Tadano, R. Takeda, H. Miyagawa, Three dimensional gait analysis using wearable acceleration and gyro sensors based on quaternion calculations, Sensors 13 (2013) 9321–9343, http://dx.doi.org/10.3390/s130709321.
[61] J.C. Alvarez, D. Alvarez, A. López, R.C. González, Pedestrian navigation based on a waist-worn inertial sensor, Sensors 12 (2012) 10536–10549, http://dx.doi.org/10.3390/s120810536.
[62] A.R. Jimenez, F. Seco, C. Prieto, J. Guevara, A comparison of Pedestrian Dead-Reckoning algorithms using a low-cost MEMS IMU, IEEE International Symposium on Intelligent Signal Processing 2009 (2009) 37–42 WISP 10.1109/WISP.2009.5286542.
[63] F. Dadashi, B. Mariani, S. Rochat, C.J. Büla, B. Santos-Eggimann, K. Aminian, Gait and foot clearance parameters obtained using shoe-worn inertial sensors in a large-population sample of older adults, Sensors 14 (2013) 443–457, http://dx.doi.org/10.3390/s140100443.
[64] A. Cretual, K. Bervet, L. Ballaz, Gillette gait index in adults, Gait Posture 32 (2010) 307–310, http://dx.doi.org/10.1016/j.gaitpost.2010.05.015.
[65] L.M. Schutte, U. Narayanan, J.L. Stout, P. Selber, J.R. Gage, M.H. Schwartz, An index for quantifying deviations from normal gait, Gait Posture 11 (2000) 25–31, http://dx.doi.org/10.1016/S0966-6362(99)00047-8.
[67] R. De Maesschalck, D. Jouan-Rimbaud, D.L. Massart, The Mahalanobis distance, Chemom. Intell. Lab. Syst. 50 (2000) 1–18, http://dx.doi.org/10.1016/S0169-7439(99)00047-7.
[68] R. Stirling, K. Fyfe, G. Lachapelle, Evaluation of a new method of heading estimation for pedestrian dead reckoning using shoe mounted sensors, J. Navig. 58 (2005) 31–45, http://dx.doi.org/10.1017/S0373463304003066.
[69] R. Harle, A survey of indoor inertial positioning systems for pedestrians, IEEE Communications Surveys & Tutorials. 15 (2013) 1281–1293, http://dx.doi.org/10.1109/SURV.2012.121912.00075.
[70] J.M. Hausdorff, D.A. Rios, H.K. Edelberg, Gait variability and fall risk in community-living older adults: a 1-year prospective study, Arch. Phys. Med. Rehabil. 82 (2001) 1050–1056, http://dx.doi.org/10.1053/apmr.2001.24893.
[71] C.S. Sterke, E.F. van Beeck, C.W.N. Looman, R.W. Kressig, T.J.M. van der Cammen, An electronic walkway can predict short-term fall risk in nursing home residents with dementia, Gait Posture 36 (2012) 95–101, http://dx.doi.org/10.1016/j.gaitpost.2012.01.012.
[72] C.R. Garman, C.T. Franck, M.A. Nussbaum, M.L. Madigan, A bootstrapping method to assess the influence of age, obesity, gender, and gait speed on probability of tripping as a function of obstacle height, J. Biomech. 48 (2015) 1229–1232, http://dx.doi.org/10.1016/j.jbiomech.2015.01.031.
[73] S. Zhang, K. Sulankivi, M. Kiviniemi, I. Romo, C.M. Eastman, J. Teizer, BIM-based fall hazard identification and prevention in construction safety planning, Saf. Sci. 72 (2015) 31–45, http://dx.doi.org/10.1016/j.ssci.2014.08.001.

Further reading

[66] M.H. Schwartz, A. Rozumalski, The gait deviation index: a new comprehensive index of gait pathology, Gait Posture 28 (2008) 351–357, http://dx.doi.org/10.1016/j.gaitpost.2008.05.001.